



The Corrosive Effect of Atmospheric Environment on Simulated Materials of Bronze Cultural Relics

Li Zhan ^{1,*} and Yan Li Jiang ¹

<https://doi.org/10.64486/m.65.4.10>

¹ Harbin University, Harbin City, No. 109 Zhongxing Avenue Nangang District, Heilongjiang Province China, 150086; jylzhl@163.com

* Correspondence: zhanli@hrbu.edu.cn

Type of the Paper: Article

Received: January 7, 2026

Accepted: March 31, 2026

Abstract: This study takes simulated materials of bronze cultural relics (copper-tin alloy-plated quartz crystal oscillators) as the research object, adopts the Quartz Crystal Microbalance (QCM) technology, and systematically investigates the effects of different temperature and humidity conditions on their corrosion. Three temperature levels (20 °C, 25 °C, and 30 °C) and corresponding gradient levels of relative humidity were set in the experiment. By monitoring the changes in frequency and mass of the quartz crystal oscillators, the corrosion kinetic rules were analyzed. The results show that temperature and humidity exert a significant influence on the corrosion of the simulated materials: under constant temperature, the higher the relative humidity, the thicker the water film on the metal surface, the greater the dissolved amount of pollutants, and the faster the corrosion rate; under constant humidity, an increase in temperature will accelerate the corrosion reaction, and the higher the relative humidity, the more pronounced the accelerating effect of temperature. Based on the experimental data, a classification standard for temperature and humidity levels was formulated. It is recommended that the long-term storage environment of bronze cultural relics in museums should be controlled at a temperature of (20–25) °C and a relative humidity below 60 %. The conclusions of this study provide a scientific basis for museums in tourist scenarios to precisely regulate temperature and humidity, optimize passenger flow management, and improve protection measures, thereby facilitating the achievement of a win-win situation for the coordinated and sustainable development of bronze cultural relic protection and the tourism industry.

Keywords: bronze cultural relic simulation materials; temperature and humidity; corrosion; quartz crystal microbalance; cultural relic protection

1. Introduction

With the vigorous development of the cultural tourism industry, bronze cultural relic sites and museums have evolved into popular tourist destinations [1]. However, environmental disturbances caused by tourist gatherings (such as heat emission from human respiration and fluctuations in temperature and humidity in crowded areas) have rendered the balance between tourism development and cultural relic protection increasingly prominent [2], emerging as a key research direction jointly concerned by the tourism and cultural heritage conservation sectors [3].

As non-renewable precious heritage carrying diverse civilizations, existing bronze cultural relic collections are generally confronted with the threat of corrosion [4]. The atmospheric corrosion of bronze in museum environments is a synergistic electrochemical process driven by multiple factors, and it is rarely induced by a single factor such as humidity alone [5]. Gaseous and particulate atmospheric pollutants widely existing in the museum microenvironment (e.g., hydrogen sulfide H_2S , sulfur dioxide SO_2 , chloride ions Cl^- , nitrogen oxides NO_x , and short-chain volatile organic acids) are core inducers of bronze corrosion [6]. These pollutants can break the passive film on the bronze surface, react with the copper-tin alloy matrix to form unstable corrosive products, and even trigger irreversible "bronze disease" under specific conditions. Among the contributing factors, temperature and humidity in the museum's atmospheric environment are the core environmental elements that induce or accelerate corrosion [7]: humidity provides a necessary liquid medium for the dissolution and electrochemical reaction of pollutants on the bronze surface, while temperature regulates the reaction rate of pollutant dissolution and corrosion [8]. Changes in temperature and humidity directly affect the formation and stability of water films on the bronze surface, thereby enhancing the corrosive effect of pollutants and triggering corrosion reactions—a problem that is even more pronounced in crowded scenarios during peak tourist seasons [5–7]. Tourist gatherings lead to local accumulation of pollutants and abnormal fluctuations of temperature and humidity, further amplifying the synergistic corrosion effect of humidity and pollutants [9].

The core orientation of this study is to solve the problem of bronze cultural relic protection in museums under tourism scenarios—tourist gatherings during peak seasons can cause intense and rapid fluctuations in local temperature and humidity in museums, which is a specific environmental disturbance that distinguishes tourism scenarios from conventional museum environments. In contrast, the concentration of pollutants such as hydrogen sulfide in museums is usually at a low and relatively stable level (museums control pollutant content through ventilation, purification and other measures, and there will be no drastic changes due to tourist activities in the short term) [10]. Therefore, this study prioritizes focusing on the specific environmental factor (temperature and humidity fluctuations) under tourism scenarios, clarifies the quantitative influence law of temperature and humidity fluctuations on bronze corrosion, and provides direct scientific basis for museums to protect cultural relics by regulating temperature and humidity and optimizing passenger flow during peak tourist seasons. Pollutants, as conventional environmental factors, are not the core issue to be solved in this study.

Most existing studies focus on the corrosion mechanism of bronze under conventional environments and have confirmed the synergistic corrosion effect of humidity and various pollutants on bronze materials, but few explore the specific impacts of temperature and humidity fluctuations associated with tourism activities on bronze cultural relics by integrating the characteristics of tourism scenarios [11]. This study focuses on investigating the impact of temperature and humidity on bronze corrosion without additional control of pollutant variables, which is a research design based on the actual microenvironmental characteristics of museums and the core scientific issues of this study, rather than ignoring the role of pollutants. Consequently, existing studies are difficult to provide targeted guidance for the protection of cultural relics in museums with tourism activities [12].

For this reason, aiming to promote the coordinated development of tourism development and cultural relic protection, this study systematically investigates the corrosion effects of temperature and humidity factors in the atmospheric environment on bronze cultural relic simulation materials by means of the reactive detection method of Quartz Crystal Microbalance (QCM). The experiment is carried out in the ambient air of the actual low-pollution microenvironment of the museum, with trace pollutants as the constant background factor, to reveal the corrosion kinetic laws under different temperature and humidity conditions and clarify the correlation characteristics between temperature and humidity fluctuations and corrosion risks. This study can provide a scientific basis for museums to precisely control temperature and humidity levels during peak tourist seasons and balance tourist experience with cultural relic protection, further refining the theoretical and practical system for the protection of bronze cultural relics in tourism scenarios.

2. Experimental Materials and Methods

2.1 Preparation of Copper-Tin Alloy Plated Quartz Crystal Resonators

AT-cut quartz crystal resonators were selected as the substrate with a fundamental frequency of 9.216 MHz, and copper-tin alloy bronze simulated coatings were prepared via electroplating; no other metal layers were pre-deposited on the surface of the resonators, the copper-tin alloy bronze coating was directly electrodeposited on the clean quartz crystal electrode surface to ensure that the frequency and mass response of the resonators could directly reflect the corrosion behavior of the bronze material. The resonators had an overall area of ~ 0.50 cm² and an effective electrode area of ~ 0.20 cm², and the AT-cut structure endowed the resonators with excellent temperature stability, which could minimize the interference of temperature drift on the experimental detection results of corrosion behavior. A QCM922 quartz crystal microbalance was used for measurement in the experiment, and its manufacturer was Ametek, Inc. (USA).

Prior to electroplating, the resonators were rigorously pretreated: sequentially rinsed with acetone, absolute ethanol, and deionized water to remove oil stains and impurities, then blow-dried with air and stored in a clean environment for use.

The electroplating bath was composed of 9.0 g/L copper sulfate, 18.4 g/L (10.0 mL/L) concentrated sulfuric acid, 4.0 g/L stannous sulfate, 2.0 g/L EDTA-Na₂, and 14.0 g/L tartaric acid. Herein, copper sulfate and stannous sulfate served as metal ion sources, concentrated sulfuric acid adjusted the bath composition, EDTA-Na₂ acted as a complexing agent to precisely control the deposition potential for the target Cu-Sn ratio, and tartaric acid improved system stability. The bath was prepared by mixing two prefabricated solutions [13]:

Solution A: Copper sulfate dissolved in deionized water at the specified concentration, stirred until fully clarified.

Solution B: Concentrated sulfuric acid diluted first, followed by slow addition of stannous sulfate with continuous stirring (Note: Direct dissolution of stannous sulfate in water is prohibited to avoid hydrolysis-induced turbidity affecting electroplating efficiency). After complete dissolution of stannous sulfate, calculated amounts of tartaric acid and EDTA-Na₂ were added sequentially, with further stirring until a homogeneous and transparent system was achieved. Solution B was then slowly poured into Solution A, thoroughly mixed, and supplemented with deionized water to the specified volume. The mixture was left to stand for degassing before use.

For electroplating, pretreated blank resonators (cathode) and copper wires (anode) were fixed with electrode clamps and immersed in the prepared bath. A potentiostat/galvanostat regulated the electroplating parameters at a current density of 3 mA/cm² for 3.0 min. After deposition, the coated resonators were immediately rinsed with deionized water to remove residual bath solution, blow-dried with nitrogen, and sealed for subsequent corrosion experiments. The chemical composition, surface morphology, and microstructural characteristics of the bronze coating were analyzed using energy-dispersive spectroscopy (EDS) and scanning electron microscopy (SEM).

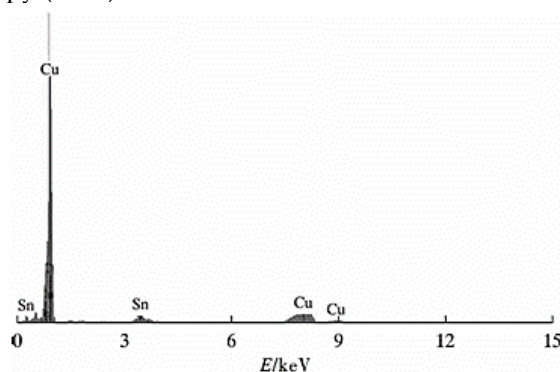
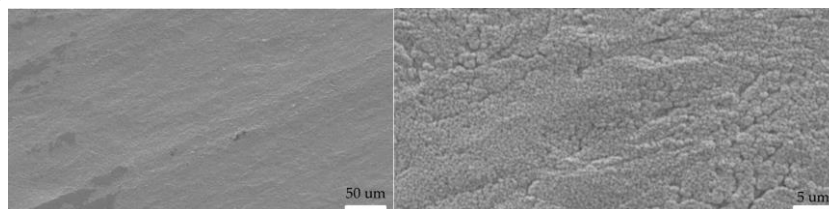


Figure 1. Energy Dispersive Spectroscopy (EDS) Spectrum of Electroplated Copper-Tin Alloy

The elemental analysis results in Figure 1 show that the copper content in the copper-tin alloy coating is 83.31 % and the tin content is 16.69 %, which is consistent with the composition of traditional tin-bronze cultural relics. This ensures the effectiveness of the coating in simulating the material of actual bronze cultural relics. No other impurity elements are detected in the coating, indicating that the electroplating system is of high purity and the bath formulation can effectively avoid the introduction of foreign impurities during the deposition process.

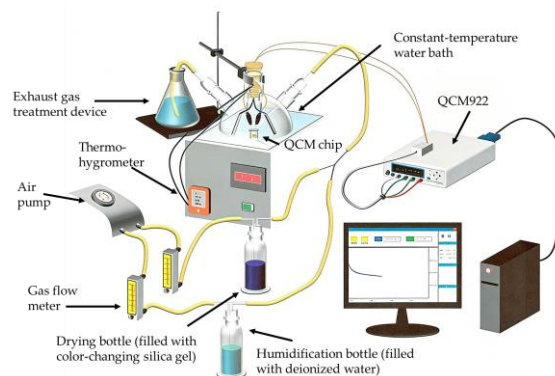
**Figure 2.** SEM image of the electrodeposited Cu-Sn alloy coating

As shown in the SEM observations in Figure 2, the Cu-Sn alloy coating exhibits a dense and uniform nodular crystalline structure, with no obvious pinholes, cracks, or loose agglomeration observed on the surface. The grains are fine and uniformly distributed.

This is consistent with the dense structural characteristics of the corrosion layers found on well-preserved bronze cultural relics, ensuring that the corrosion behavior of the simulated coating can reflect the corrosion laws of actual bronze cultural relics in an atmospheric environment.

2.2 QCM Reactive Monitoring Experiments

As shown in Figure 3, a 3-L four-necked flask was used as the corrosion reaction vessel for the resonators, with a constant-temperature water bath maintaining the internal temperature to ensure experimental stability. Air was introduced into the flask via an air pump, configured with two separate channels (dry and wet): the dry air channel utilized color-changing silica gel to adsorb moisture for dry air, while the wet air channel humidified air with deionized water to generate moist air. Flow meters precisely regulated the flow rates of the two air streams for controllable adjustment of internal relative humidity (RH), and real-time temperature and RH were monitored and recorded using a thermo-hygrometer. A computer collected the resonators' frequency signals at 10-s intervals, with 40 h of continuous acquisition per experiment to capture dynamic frequency changes during corrosion.

**Figure 3.** Schematic diagram of the QCM in-situ monitoring experimental setup

To investigate the effects of different temperature and RH conditions on the corrosion behavior of the bronze simulated materials, multiple sets of variable experiments were designed. The specific parameters are as follows: at 20 °C, RH = 40 %, 50 %, 60 %, 70 %, 90 %; at 25 °C, RH = 40 %, 50 %, 60 %, 70 %, 90 %; and at 30 °C, RH = 40 %, 50 %, 60 %, 70 %, 80 %.

3. Experimental Results and Discussion

According to existing research, ambient temperature affects the chemical reaction rate on metal surfaces and the solubility of soluble pollutants, while humidity impacts the formation, condensation thickness, and residence time of liquid films on the surface of metal materials. The corrosion of bronze cultural relics is largely influenced by the combined effect of temperature and humidity [14]. Therefore, it is necessary to explore the optimal temperature and humidity range for the preservation of bronze cultural relics in museum atmospheric environments by studying the effects of different temperature and humidity conditions on the corrosion of simulated materials for bronze cultural relics.

The environmental conditions controlled in the experiment were as follows: relative humidity (RH) of 40 %, 50 %, 60 %, 70 %, and 90 % at temperatures of 20 °C and 25 °C, and RH of 40 %, 50 %, 60 %, 70 %, and 80 % at a temperature of 30 °C. The corrosion behavior of the simulated materials for bronze cultural relics was investigated by monitoring the frequency change (Δf) of copper-tin alloy-plated quartz crystal oscillators under different temperature and humidity conditions, which reflects the surface mass change (Δm).

Based on the Sauerbery equation (Equation 1), the mass change of the copper-tin alloy-plated quartz crystal oscillators under different environmental conditions can be calculated from their frequency change:

$$\Delta f = \frac{-2f_0^2}{A \cdot (\mu\rho)^{\frac{1}{2}}} \Delta m \quad (1)$$

Where:

f = natural frequency of the quartz crystal oscillator/Hz

A = area of the metal film plated on the surface of the crystal oscillator/cm²

μ = shear modulus of quartz, with a value of $2.947 \times 10^{11} \text{ g} \cdot \text{cm} \cdot \text{s}^{-2}$

ρ = density of quartz, with a value of $2.648 \text{ g} \cdot \text{cm}^{-3}$.

The fundamental frequency of the quartz crystal oscillators used in the experiment was 9.216 MHz, and the area of the metal film plated on their surface was approximately 0.40 cm². The conversion formula for calculating the mass change Δm is derived as follows:

$$\Delta m = -2.08 \times 10^{-9} \Delta f \quad (2)$$

The curves of frequency change and mass change over time for the copper-tin alloy-plated quartz crystal oscillators under different humidity conditions at 20 °C, 25 °C, and 30 °C are shown in Figure 4. As can be seen from the figure, the resonant frequency of the crystal oscillators showed a decreasing trend under all experimental conditions [15]. According to the Sauerbery equation, this indicates that the mass of the copper-tin alloy-plated crystal oscillators increased with prolonged exposure time. This phenomenon can be attributed to two main factors: first, water molecules condensed on the surface of the crystal oscillators to form a water film, and the increase in water film thickness led to an increase in the surface mass of the oscillators; second, the electrodeposited copper-tin alloy on the surface of the crystal oscillators underwent corrosion, and the continuous accumulation of corrosion products on the alloy surface further increased the surface mass of the oscillators [16]. At the same temperature, during the initial stage of exposure, both the magnitude of frequency decrease per unit time and the magnitude of mass increase per unit time of the crystal oscillators increased with the rise in humidity. This suggests that atmospheric humidity can affect the rate and thickness of water film condensation on the surface of the copper-tin alloy: the higher the humidity, the faster the formation of the water film on the alloy surface and the thicker the condensed water film. In environments with higher humidity, the water film condensation rate on the crystal oscillators was faster than that in low-humidity environments, implying that the copper-tin alloy plating on the surface might initiate corrosion reactions more rapidly in the early stage of exposure due to the quick formation of the water film [17].

In general, the slope of frequency decrease and the slope of mass increase of the crystal oscillators were relatively large in the early stage of exposure. With the extension of exposure time, the variation range of these

slopes gradually decreased and tended to stabilize. This may be because water film condensation proceeded rapidly in the early stage, leading to a fast increase in the surface mass of the crystal oscillators. Once the water film thickness ceased to increase, the magnitude of frequency decrease of the crystal oscillators remained almost constant, which was mainly due to the corrosion of the copper-tin alloy plating and the gradual accumulation of corrosion products.

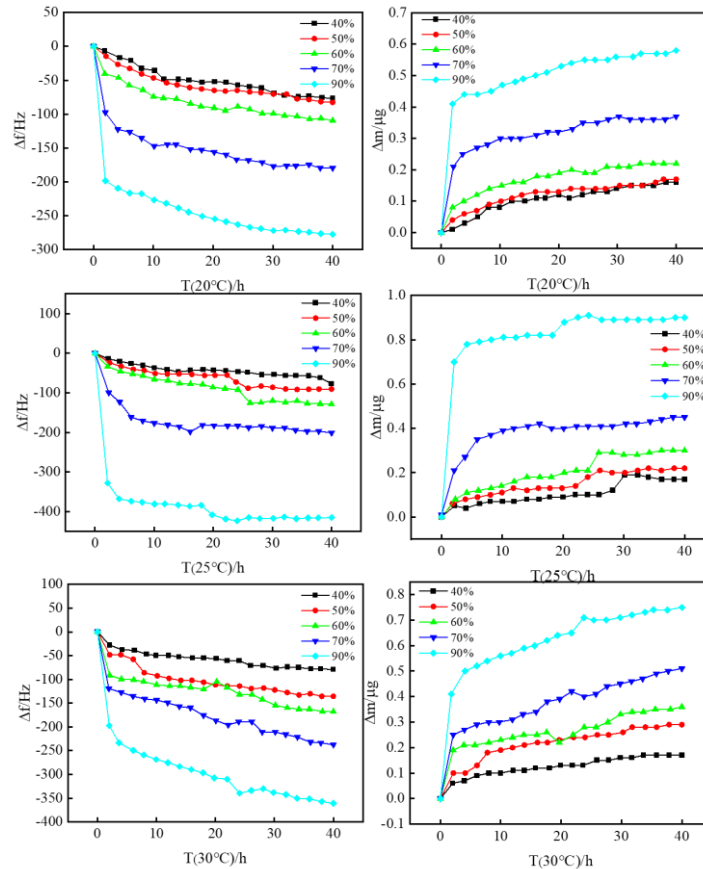


Figure 4. Curves of frequency and mass changes over time for copper-tin alloy-plated quartz crystal oscillators under different humidity conditions at 20 °C, 25 °C, and 30 °C

Figure 5 presents the frequency change values of copper-tin alloy-plated quartz crystal oscillators following 40 hours of exposure in environments with varying temperatures. Meanwhile, the frequency change values and calculated mass change values of these oscillators after 40 hours of exposure under different temperature and humidity conditions are summarized in Table 1.

By correlating the curves in Figure 5 with the frequency change values in Table 1, a clear trend emerges: under the same relative humidity, higher temperatures correspond to greater frequency decreases and mass increases in the copper-tin alloy-plated quartz crystal oscillators. This observation indicates that elevated temperatures accelerate the corrosion of the copper-tin alloy coating on the oscillator surface and promote the formation of corrosion products. Consequently, a larger quantity of corrosion products accumulates on the oscillator surface over the same exposure period [18].

Further analysis of Figure 2 reveals an additional relationship: the greater the environmental relative humidity, the larger the disparity in frequency change values among the three tested temperatures. This finding suggests that temperature exerts a minimal influence on the corrosion rate of copper-tin alloy at low relative humidity. In contrast, as relative humidity increases, the impact of temperature on the atmospheric corrosion of copper-tin alloy becomes increasingly pronounced [19].

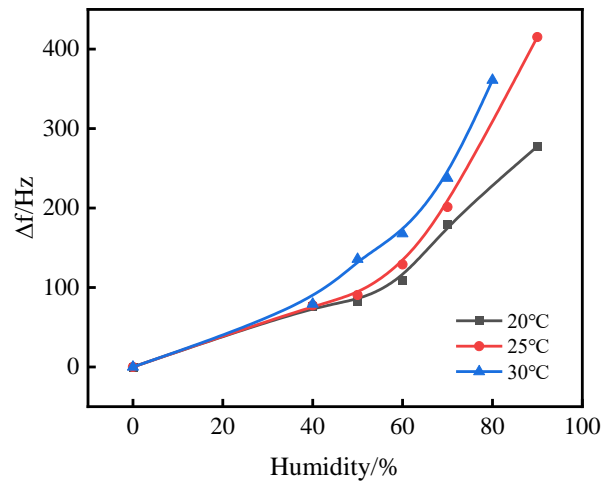


Figure 5. Frequency change values of copper-tin alloy-plated quartz crystal oscillators after 40 h of exposure under different temperature and humidity conditions

Table 1. Frequency variation values and mass variation amounts of copper-tin plated crystal oscillator plates after 40 h exposure under different temperature and humidity conditions

Temperature /°C	Humidity /%	$ \Delta f /\text{Hz}$	$\Delta m/\mu\text{g}$
20	40	76.78	0.16
	50	82.72	0.17
	60	109.43	0.22
	70	179.61	0.37
	90	277.51	0.58
25	40	77.41	0.17
	50	90.43	0.22
	60	128.98	0.3
	70	201.34	0.45
	90	415.26	0.90
30	40	79.19	0.17
	50	135.57	0.29
	60	167.79	0.36
	70	237.58	0.51
	80	361.07	0.75

The thickness of the water film condensed on the metal surface exerts a crucial impact on metal corrosion. Under low humidity conditions, the thin water film on the metal surface dissolves fewer pollutants, resulting in mild corrosion of the metal surface. As the relative humidity rises, the water film on the metal surface thickens, and more pollutants in the air dissolve in the water film, which causes more severe metal corrosion. To better classify the corrosion degree of simulated bronze cultural relic materials under different temperature and humidity conditions, the average corrosion depth per unit time is adopted to calculate the metal corrosion rate.

The quartz crystal microbalance (QCM) method is essentially a mass gain method, a common technique for measuring metal corrosion rate. It is usually expressed as the mass gain per unit area of metal per unit time, with the specific formula as follows:

$$v = \frac{\Delta m}{A \cdot t} = \frac{m_1 - m_0}{A \cdot t} \quad (3)$$

Where:

v = corrosion rate of the metal specimen/(g/(cm⁻² · h))

m_1 = weight of the metal specimen after corrosion/g

m_0 = weight of the metal specimen before corrosion/g

A = surface area of the metal specimen/cm²

t = corrosion duration/h.

The conversion formula for expressing the metal corrosion rate by corrosion depth is:

$$d = \frac{87600v}{\rho} \quad (4)$$

Where:

d = metal corrosion depth rate (mm/a);

ρ = density of the metal (g·cm⁻³).

It is known that the exposed surface area of the metal in the experiment is 0.40 cm², the exposure time is 40 h, and the density of bronze is 8.75 g·cm⁻³. Substituting the above parameters into the formula, the derived result is obtained as follows:

$$d = 2.856\Delta m \quad (5)$$

Where:

d = metal corrosion depth rate/(nm/40h)

Δm = mass loss of the specimen/μg.

The corrosion rate was calculated directly from the total mass increment monitored by QCM, without deducting the initial mass contribution of water film condensation. This approach is justified by three key scientific considerations: (1) The condensed water film, as a prerequisite for atmospheric corrosion, reaches a gas-solid dynamic equilibrium rapidly after initial formation, thus acting as a constant baseline that does not affect the relative corrosion rate calculation. (2) In the low-pollution museum microenvironment, the mass of the initial water film is negligible, especially at high relative humidities where corrosion risk is critical.

The initial stage of the frequency shift curve (0–2 h) provided direct experimental evidence for the relationship between humidity and water film thickness. At constant temperature, the magnitude of the initial frequency drop was positively correlated with relative humidity. For instance, at 20 °C, the initial frequency decrease at 90 % RH was significantly larger than that at 40 % RH. According to the Sauerbrey equation, this directly indicates that higher relative humidity leads to a greater mass of condensed water film on the oscillator surface, confirming the formation of a thicker liquid film under high-humidity conditions.

Based on the air cleanliness and pollution classification standard proposed by Puraf Corporation (USA), with the copper corrosion rate C₁ standard (<9 nm/30d) as the reference, the recommended range for the classification of environmental temperature and humidity for the preservation of collection bronze cultural relics was put forward [20]:

Level 1 (Safe range): < 7 nm/30d

Level 2 (Relatively safe range): < 9 nm/30d

Level 3 (Permissible range): < 15 nm/30d

Level 4 (Critical range): < 25 nm/30d

Level 5 (Hazardous range): > 25 nm/30d.

The corrosion rates of the simulated bronze cultural relic materials under different temperature and humidity conditions were calculated according to Formula 5, and the results are listed in Table 2. Figure 6 shows the corrosion rate curve of the simulated bronze cultural relic materials exposed under different temperature and humidity conditions. According to the corrosion rate curve in Figure 6 and the formulated classification basis, a recommended grading diagram for the temperature and humidity environment for the preservation of bronze cultural relics in museums was proposed.

Figure 7 presents the recommended temperature and humidity classification map for bronze cultural relic preservation in museums. As indicated in the figure, the environmental temperature and humidity for bronze relic preservation should be controlled within Grade 3 for most of the time. When the temperature and humidity fall into the Grade 4 critical range, adjustment should be made promptly to avoid damage to the cultural relics. In addition, it can be seen from the classification map that the lower the temperature, the wider the suitable environmental humidity range for bronze cultural relic preservation. Therefore, the indoor temperature of the museum should not be too high during temperature regulation.

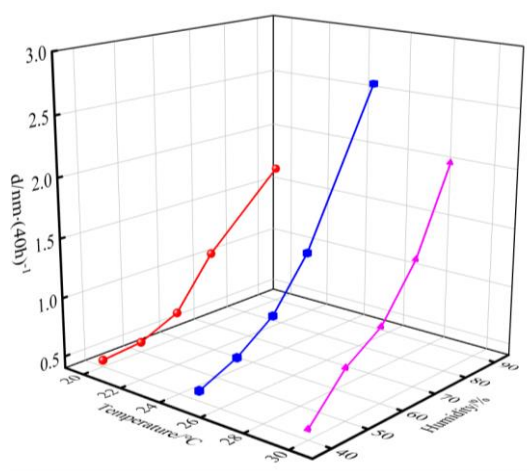


Figure 6. Corrosion rate curves of simulated bronze cultural relic materials under different temperature and humidity conditions

Table 2. Corrosion rate of simulated bronze cultural relic materials exposed under different temperature and humidity conditions

Temperature/°C	Humidity/%	d/nm (40 h) ⁻¹
20	40	0.457
	50	0.486
	60	0.628
	70	1.057
	90	1.656
25	40	0.486
	50	0.628
	60	0.857
	70	1.285
	90	2.570
30	40	0.486
	50	0.828
	60	1.028

70	1.457
80	2.142

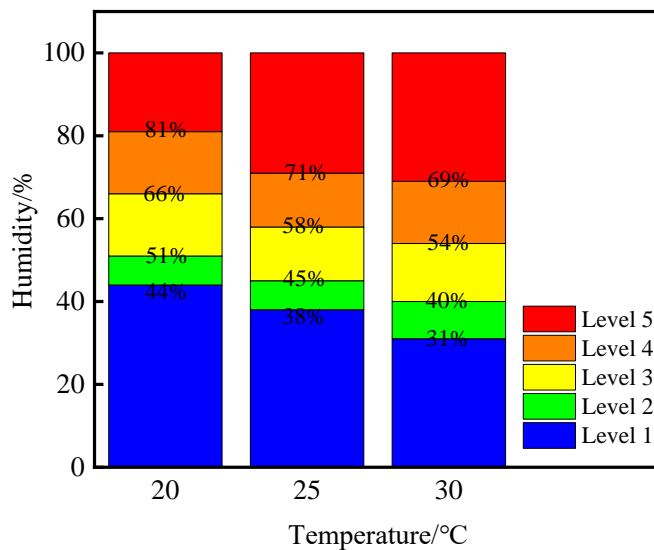


Figure 7. Suggested diagram for temperature and humidity grade classification of bronze cultural relics preservation in museums

4. Conclusion

The experimental results show that the environmental temperature and humidity have a significant impact on the corrosion of the simulated materials for bronze artifacts. When the environmental temperature is constant, the higher the relative humidity, the more pollutants in the atmosphere can dissolve into the liquid film on the metal surface, accelerating the corrosion rate of the electroplated copper-tin alloy and causing an increase in the surface quality of the crystal oscillator plate; when the relative humidity is constant, an increase in temperature will promote the corrosion reaction of the copper-tin alloy, resulting in an increase in corrosion products and also causing an increase in the surface quality of the crystal oscillator plate. Among them, when the relative humidity is low, the influence of temperature on the corrosion of the copper-tin alloy is weak; while the higher the relative humidity, the more obvious the aggravating effect of temperature on the corrosion of the coating. Combined with the experimental data and the recommended diagram for the temperature and humidity levels of bronze artifacts in museums, the temperature and humidity of the storage environment for the museum's bronze artifacts should be maintained at (20–25) °C and below 60 % relative humidity for a long time. This parameter standard has important guiding significance for the protection of cultural relics in tourism scenarios.

References

- [1] J. Thunberg, N. Emmerson and D. Watkinson, "New evidence of the relationship between oxidative hydrolysis of CuCl 'bronze disease' and relative humidity (RH) for management of archaeological copper alloys," *Heritage*, vol. 8, no. 9, art. no. 350, 2025, <https://doi.org/10.3390/heritage8090350>
- [2] T. de Caro et al., "Roman and Early Medieval bronze artifacts from the Middle Tiber Valley: Technological and conservation insight through optical microscopy, Raman spectroscopy, SEM-EDS, and electrochemical analysis," *Archaeological and Anthropological Sciences*, vol. 18, art. no. 27, 2026, <https://doi.org/10.1007/s12520-025-02384-3>

- [3] H. Li et al., "Research Progress on Characterization Techniques for the Corrosion Behavior of Bronze Artifacts," *Materials*, vol. 19, no. 1, art. no. 162, 2026, <https://doi.org/10.3390/ma19010162>
- [4] G. Artioli et al., "The tin content of lead inclusions in ancient tin-bronze artifacts: a time-dependent process," *Journal of Applied Crystallography*, vol. 57, no. 3, pp. 700–706, 2024, <https://doi.org/10.1107/S1600576724002218>
- [5] D. A. Scott, "Bronze disease: a review of some chemical problems and the role of relative humidity," *Journal of the American Institute for Conservation*, vol. 29, no. 2, pp. 193–206, 1990, <https://doi.org/10.1179/019713690806046064>
- [6] F. Samie et al., "Atmospheric corrosion effects of HNO₃—Influence of temperature and relative humidity on laboratory-exposed copper," *Atmospheric Environment*, vol. 41, no. 7, pp. 1374–1382, 2007, <https://doi.org/10.1016/j.atmosenv.2006.10.018>
- [7] S. Bradley, "Preventive conservation research and practice at the British Museum," *Journal of the American Institute for Conservation*, vol. 44, no. 3, pp. 159–173, 2005, <https://doi.org/10.1179/019713605806082248>
- [8] M. A. Petrunin et al., "Application of the quartz crystal microbalance technique in corrosion studies: A review," *International Journal of Corrosion and Scale Inhibition*, vol. 9, no. 1, pp. 92–117, 2020, <https://doi.org/10.17675/2305-6894-2020-9-1-6>
- [9] M. Forslund and C. Leygraf, "A quartz crystal microbalance probe developed for outdoor in situ atmospheric corrosivity monitoring," *Journal of The Electrochemical Society*, vol. 143, no. 3, pp. 839–844, 1996, <https://doi.org/10.1149/1.1836546>
- [10] S. Zakipour and C. Leygraf, "Quartz crystal microbalance applied to studies of atmospheric corrosion of metals," *British Corrosion Journal*, vol. 27, no. 4, pp. 295–298, 1992, <https://doi.org/10.1179/bcj.1992.27.4.295>
- [11] T. Prošek et al., "Application of automated electrical resistance sensors for measurement of corrosion rate of copper, bronze and iron in model indoor atmospheres containing short-chain volatile carboxylic acids," *Corrosion Science*, vol. 87, pp. 376–382, 2014, <https://doi.org/10.1016/j.corsci.2014.06.047>
- [12] Z. Wang et al., "Research progress on ancient bronze corrosion in different environments and using different conservation techniques: a review," *MRS Advances*, vol. 2, no. 37–38, pp. 2033–2041, 2017, <https://doi.org/10.1557/adv.2017.222>
- [13] R. L. Sacci et al., "Copper-Tin Alloys for the Electrocatalytic Reduction of CO₂ in an Imidazolium-Based Non-Aqueous Electrolyte," *Energies*, vol. 12, no. 16, art. no. 3132, 2019, <https://doi.org/10.3390/en12163132>
- [14] K. Popova and T. Prošek, "Corrosion monitoring in atmospheric conditions: a review," *Metals*, vol. 12, no. 2, art. no. 171, 2022, <https://doi.org/10.3390/met12020171>
- [15] K. Singla et al., "Quantification of the adsorption kinetics of a model corrosion inhibitor on gold using QCM-D," *Corrosion*, vol. 80, no. 12, pp. 1207–1215, 2024, <https://doi.org/10.5006/4634>
- [16] H. Pu and X. Wang, "The impact of environment on cultural relics," *Scientific Culture*, vol. 9, no. 2, pp. 49–62, 2023, <https://doi.org/10.5281/zenodo.7918252>
- [17] H. Li et al., "Recent progress on corrosion behavior, mechanism, and protection strategies of bronze artefacts," *Heritage*, vol. 8, no. 8, art. no. 340, 2025, <https://doi.org/10.3390/heritage8080340>
- [18] H. Luo et al., "Influence of the aging time on the microstructure and electrochemical behaviour of a 15-5PH ultra-high strength stainless steel," *Corrosion Science*, vol. 139, pp. 185–196, 2018, <https://doi.org/10.1016/j.corsci.2018.04.032>
- [19] H. B. Gunay, O. B. Isgor and P. Ghods, "Kinetics of passivation and chloride-induced depassivation of iron in simulated concrete pore solutions using electrochemical quartz crystal nanobalance," *Corrosion*, vol. 71, no. 5, pp. 615–627, 2015, <https://doi.org/10.5006/1346>
- [20] N. S. Baer and P. N. Banks, "Conservation notes: Environmental standards," *International Journal of Museum Management and Curatorship*, vol. 6, no. 2, pp. 207–209, 1987, <https://doi.org/10.1080/09647778709515068>